Parity assignments in ^{140}Ce up to 7 MeV using Compton polarimetry

M. A. Büssing, M. Elvers, J. Endres, J. Hasper, and A. Zilges
Institut für Kernphysik, Universität zu Köln, D-50937 Köln, Germany

M. Fritzsche, K. Lindenberg, S. Müller, D. Savran, and K. Sonnabend
Institut für Kernphysik, TU Darmstadt, D-64289 Darmstadt, Germany
(Received 21 July 2008; published 14 October 2008)

Parity quantum numbers of $J = 1$ states up to 7 MeV in the region of the Pygmy Dipole Resonance in ^{140}Ce were determined model independently by combining the methods of Nuclear Resonance Fluorescence and Compton polarimetry. For the first time the well-established method of Compton polarimetry was applied at such high energies. The experiment was performed using a fourfold segmented HPGe clover detector for the detection of the scattered photons. For all investigated dipole transitions asymmetries are found which correspond to negative parity of the excited states.

DOI: 10.1103/PhysRevC.78.044309 PACS number(s): 21.10.−k, 24.70.+s, 25.20.Dc, 27.60.+j

I. INTRODUCTION

In the last decade the dipole response of atomic nuclei up to the particle separation energies has been studied systematically in various nuclei covering a wide mass range using the method of real-photon scattering [1,2]. In most medium to heavy nuclei a concentration of electric dipole strength below the neutron separation energy was observed, which is usually denoted as Pygmy Dipole Resonance (PDR), e.g., see Refs. [3–7]. Systematic studies of isotonic and isotopic chains have revealed a rather smooth development of the gross features like center of mass energy and total integrated strength of the PDR in neighboring nuclei. Therefore, the PDR is proposed as a new common mode in atomic nuclei, while its collectivity is a matter of ongoing discussions [8].

The interpretation of these excitations is in many cases based on the assumption of negative parity for the majority of $J = 1$ states between 5 and 9 MeV. Their parity was measured directly only in a few cases, e.g., using laser Compton backscattering [9]. In recent experiments the low-lying dipole excitations in ^{140}Ce were studied using the $(\alpha, \alpha'\gamma)$ reaction [10]. The results reveal a splitting of the dipole strength in ^{140}Ce: while the dipole excitations below 6 MeV were observed in $(\alpha, \alpha'\gamma)$ as well as in (γ, γ') experiments, the excitations above 6 MeV could only be observed in (γ, γ') experiments. Under the given kinematic conditions of forward-angle scattering under 3.5° and a beam energy of $E_\alpha = 136$ MeV Coulomb excitation is suppressed. In first order, a reaction with spinless projectile and target only populates natural parity states via nuclear scattering [11]. So a simple explanation for the nonobservation of the higher-lying states could be that they have positive parity. The aim of the present work is therefore to determine the parity of the high-lying dipole states in ^{140}Ce in a model-independent way.

The experimental method of Nuclear Resonance Fluorescence has been shown to be able to determine fundamental properties of bound $J = 1$ states. Due to the well-understood excitation mechanism and the low momentum transfer of real photons the method has a high selectivity to low-spin states and provides the possibility of extracting absolute $B(\sigma l)$ values as well as angular momenta in a model-independent way [1].

While the multipolarity of a transition radiation can be extracted from the angular distribution of the resonantly scattered photons, its electric or magnetic character can only be determined from polarization observables.

When using unpolarized photons in the entrance channel the polarization of the scattered photon contains information on the parity of the excited states. Measurements of the linear polarization using the polarization dependence of Compton scattering (generally denoted as Compton polarimetry) have proven to be a reliable tool for model-independent parity assignments at energies up to about 4 MeV [12–18]. At these energies the analyzing power of the Compton effect has dropped already significantly and reliable parity assignments become difficult [19]. To counter the strongly decreasing analyzing power and make Compton polarimetry applicable at higher energies, higher photopeak efficiencies and longer measuring times are needed.

II. EXPERIMENTAL AND THEORETICAL BASICS

A. Experimental method

The experiment was performed at the High-Intensity Photon Setup (Fig. 1) at the superconducting linear accelerator S-DALINAC for electrons at the TU Darmstadt. Unpolarized bremsstrahlung is produced by stopping the electron beam in a segmented copper radiator. Behind the radiator the bremsstrahlung beam is collimated to prepare a well-defined photon beam of about 3 cm diameter at the target positions. Following the first experimental setup with three actively shielded HPGe detectors a second target position with an additional detector could be set up. At this position a fourfold segmented HPGe clover detector is used at an angle of 90 degrees with respect to the incoming photon beam. This second measuring station provides the possibility of parasitic longtime measurements.

As in-beam targets ^{11}B, ^{32}S, ^{208}Pb, and ^{140}Ce were used. The measurement durations were 26, 74, 63, and 290 hours,

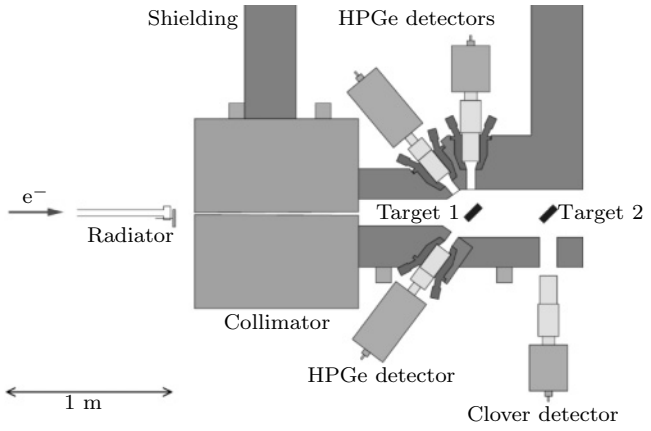

FIG. 1. High-Intensity Photon Setup at the superconducting linear accelerator for electrons S-DALINAC. The electron beam coming from the left produces bremsstrahlung photons in a copper radiator.

respectively, with average beam currents of about 20 μA. For the determination of the intrinsic asymmetry also the decay radiation of ^{56}Co and ^{60}Co sources was analyzed.

B. Basics of Compton polarimetry

For nuclear scattering processes restricted to multipolarities $L \leqslant 2$ the directional correlation between incident and scattered photons is given by

$$W(\vartheta) = \sum_{\nu=0,2,4} A_\nu(1) A_\nu(2) P_\nu(\cos\vartheta) \tag{1}$$

with the Legendre polynomials $P_\nu(\cos\vartheta)$ and the scattering angle ϑ. Restricting ourselves to two multipole components L_i and $L_i' = L_i + 1$ the expansion coefficients for the nth transition are given by [1,20]

$$A_\nu(n) = \frac{1}{1+\delta_n^2}\big[F_\nu(L_n L_n J_n J) + 2\delta_n F_\nu(L_n L_n' J_n J) + \delta_n^2 F_\nu(L_n' L_n' J_n J)\big] \tag{2}$$

with the angular momenta J_n and J of the nth state and of the intermediate state, respectively, and the mixing ratios δ_n. The coefficients are normalized so that $A_0(n) = 1$. The coefficients F_ν are listed, e.g., in Ref. [21]. Taking now into account the linear polarization of the scattered photon the correlation function $W(\vartheta, \varphi)$ can be written as

$$W(\vartheta,\varphi) = W(\vartheta) + (\pm)_{L_2'} \sum_{\nu=2,4} A_\nu(1) \times A_\nu'(2) P_\nu^{(2)}(\cos\vartheta)\cos 2\varphi \tag{3}$$

with the unnormalized associated Legendre Polynomials $P_\nu^{(2)}(\cos\vartheta)$. The polarization angle φ is defined as the angle between the reaction plane (spanned by the momentum vectors of the incoming and the scattered photon) and the polarization plane (spanned by the momentum vector of the scattered photon and its electric field vector). The factors $(\pm)_{L_2'}$ correspond to ± 1 for electric and magnetic transitions L_2', respectively. The coefficients $A_\nu'(2)$ are given by

$$A_\nu'(2) = \frac{1}{1+\delta_2^2}\big[-\kappa_\nu(L_2 L_2) F_\nu(L_2 L_2 J_2 J) + 2\delta_2 \kappa_\nu(L_2 L_2') F_\nu(L_2 L_2' J_2 J) + \delta_2^2 \kappa_\nu(L_2' L_2') F_\nu(L_2' L_2' J_2 J)\big] \tag{4}$$

with the polarization coefficients κ_ν listed, e.g., in Ref. [22]. The coefficients are normalized so that $A_0'(2) = 1$. The degree of linear polarization P_γ is usually defined as

$$P_\gamma(\vartheta) \equiv \frac{W(\vartheta,\varphi=0^\circ) - W(\vartheta,\varphi=90^\circ)}{W(\vartheta,\varphi=0^\circ) + W(\vartheta,\varphi=90^\circ)}. \tag{5}$$

With Eq. (3) this becomes

$$P_\gamma(\vartheta) = (\pm)_{L_2'} \frac{\sum_\nu A_\nu(1) A_\nu'(2) P_\nu^{(2)}(\cos\vartheta)}{\sum_\nu A_\nu(1) A_\nu(2) P_\nu(\cos\vartheta)}. \tag{6}$$

In the case of pure dipole or quadrupole transitions (spin sequences 0-1-0 and 0-2-0, respectively) and for a scattering angle of $\vartheta = 90^\circ$ full linear polarization $|P_\gamma| = 1$ is obtained, see Table I.

The linear polarization of the scattered photons can be determined by making use of the polarization dependency of the Compton scattering process. A detection system of scatterer and analyzers allows us to distinguish between Compton scattering parallel and perpendicular to the reaction plane (see Fig. 2). The asymmetry ε which is defined as

$$\varepsilon = \frac{\alpha N_\perp - N_\parallel}{\alpha N_\perp + N_\parallel} \tag{7}$$

is directly related to the degree of linear polarization P_γ by

$$\varepsilon = P_\gamma Q_\gamma(E_\gamma). \tag{8}$$

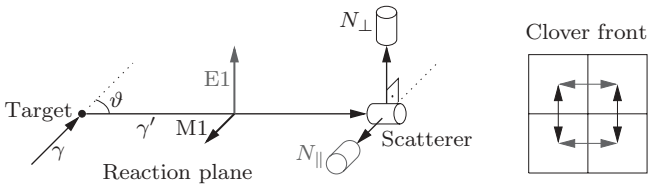

FIG. 2. Principles of Compton polarimetry. The primary photon beam γ is resonantly scattered at the target and shows a linear polarization depending on the parity of the excited state. The linear polarization of the scattered photons γ' is determined with a system of scatterer and analyzers. On the right-hand side a schematic front view of the Clover detector is shown. The arrows symbolize the coincidences between neighboring segments which define the Compton scattering plane.

TABLE I. In the case of pure dipole or quadrupole transitions maximum degree of linear polarization $|P_\gamma| = 1$ is obtained at $\vartheta = 90^\circ$. The parity of the excited state determines the sign of the degree of linear polarization.

Transition	J^π-sequence	$P_\gamma(\Theta = 90^\circ)$
$E1$	$0^+ \to 1^- \to 0^+$	-1
$M1$	$0^+ \to 1^+ \to 0^+$	$+1$
$E2$	$0^+ \to 2^+ \to 0^+$	$+1$

The parameter α in Eq. (7) includes possible intrinsic asymmetries of the detection system. The polarization sensitivity Q_γ in Eq. (8) is parametrized by

$$Q_\gamma = \frac{\frac{d\sigma}{d\Omega}(\vartheta, \varphi = 90^\circ) - \frac{d\sigma}{d\Omega}(\vartheta, \varphi = 0^\circ)}{\frac{d\sigma}{d\Omega}(\vartheta, \varphi = 90^\circ) + \frac{d\sigma}{d\Omega}(\vartheta, \varphi = 0^\circ)}(a_Q + b_Q E_\gamma), \quad (9)$$

where the first factor is the analyzing power of the Compton effect for point-like scatterer and analyzers and the second factor takes into account their finite dimensions. The differential cross sections are given by the Klein-Nishina formula and a_Q, b_Q are fit parameters. As Q_γ does not change with the character of the radiation inspected, for a given spin the sign of the asymmetry allows us to distinguish between positive and negative parity of the excited states.

III. RESULTS

A. Intrinsic asymmetry and polarization sensitivity

To allow the determination of linear polarization with a given detection system, the intrinsic asymmetry [see Eq. (8)] and the polarization sensitivity [see Eq. (6)] have to be known.

By analysis of unpolarized radiation the intrinsic asymmetry of the detection system can be determined. For this purpose ^{56}Co and ^{60}Co sources and a ^{11}B in-beam target were used. For unpolarized radiation the parameter α, which was introduced in Eq. (8) to characterize the intrinsic asymmetry, is given as the ratio of coincidences parallel and perpendicular to the reaction plane

$$\alpha(P_\gamma = 0) = \frac{N_\parallel}{N_\perp}. \quad (10)$$

This ratio is plotted in Fig. 3. By fitting a constant to the data over the entire energy range, the parameter of this fit is found to be

$$\alpha = 0.995(6). \quad (11)$$

This value is consistent with a negligible intrinsic asymmetry of $\alpha = 1$ as expected because of the compactness of the detection system.

For the determination of the polarization sensitivity, dipole and quadrupole transitions of excited states of known parity of

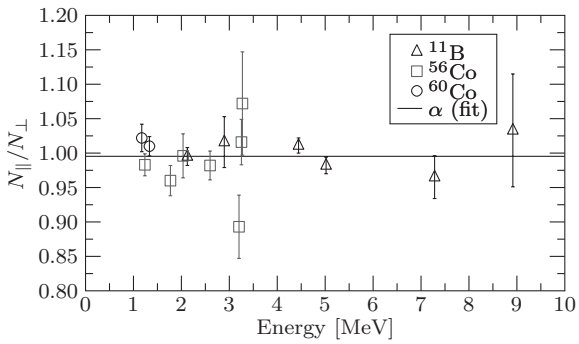

FIG. 3. Intrinsic asymmetry of the detection system. Asymmetries of decay lines of ^{56}Co and ^{60}Co sources and of excitations of ^{11}B were fitted with a constant function. An intrinsic-asymmetry parameter of $\alpha = 0.995(6)$ was obtained from the fit.

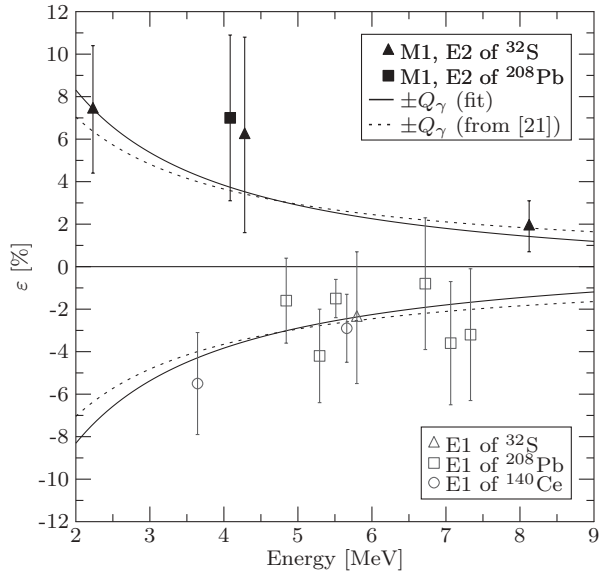

FIG. 4. Polarization sensitivity of the clover detector. Dipole and quadrupole transitions of excited states of known parity of ^{32}S, ^{208}Pb, ^{140}Ce were analyzed in terms of their asymmetry. The function from Eq. (8) was fitted to the absolute values. The fitting parameters $a_Q = 0.38(12)$ and $b_Q = -1.9(22) \times 10^{-5}$ keV^{-1} are obtained.

the nuclei ^{32}S, ^{208}Pb, and ^{140}Ce were analyzed. The parameters a_Q, b_Q in Eq. (9) were fixed as

$$a_Q = 0.38(11)$$

and

$$b_Q = -1.9(22) \times 10^{-5}\ \text{keV}^{-1}$$

see Fig. 4 and Table II. The measured polarization sensitivity is in good agreement with extrapolations of the results published in Ref. [23] which were obtained for a clover detector with similar dimensions but at lower photon energies. In the energy range between 5 and 7 MeV the polarization sensitivity accounts for 2–4%.

TABLE II. Asymmetries of electric and magnetic dipole and electric quadrupole transitions of excited states of known parity in ^{32}S, ^{208}Pb, ^{140}Ce.

Target/duration [h]	E_γ [keV]	J^π	ε [%]
^{32}S/74	2231(2)	2^+	7.4(30)
	4281(2)	2^+	6.2(46)
	5796(2)	1^-	−2.4(31)
	8124(2)	1^+	1.9(12)
^{208}Pb/63	4085(2)	2^+	7.0(39)
	4842(2)	1^-	−1.6(20)
	5293(2)	1^-	−4.2(22)
	5512(2)	1^-	−1.5(9)
	6721(2)	1^-	−0.8(31)
	7064(2)	1^-	−3.6(29)
	7332(2)	1^-	−3.2(31)
^{140}Ce/290	3644(2)	1^-	−5.5(24)
	5660(2)	1^-	−2.9(16)

TABLE III. Asymmetries for transitions in ^{140}Ce and assigned parities of the appropriate excited states. Negative parity is assigned to all states. In the cases of groups of peaks evaluated together (marked with *) the parities assigned are put in parentheses. Confidence levels for the exclusion of positive parity are also listed, see text for details. The values for $P(\chi^2)$ are expressed in units of Gaussian standard deviations. The number symbols correspond to those in Figs. 5 and 6.

Symbol	E_γ [keV]	J	ε [%]	π	Conf. [σ]	$P(\chi^2)$ [σ]
①	6119(2)	1	−7.3(4.4)	−1	2.2	2.0
②	6296(2)	1	−3.8(3.4)	−1	1.7	1.6
③	6398(2)	1	−6.8(2.4)	−1	3.7	3.2
④	6439(2)*	1	−2.6(2.7)	(−1)	1.7	1.5
	6449(2)*	1	−2.6(2.7)	(−1)	1.7	1.5
	6459(2)*	1	−2.6(2.7)	(−1)	1.7	1.5
⑤	6498(2)	1	−1.3(2.4)	−1	1.4	1.2
⑥	6537(2)	1	−3.7(2.2)	−1	2.6	2.2
⑦	6606(2)*	1	−2.6(4.2)	(−1)	1.1	1.0
	6616(2)*	1	−2.6(4.2)	(−1)	1.1	1.0
⑧	6863(2)	1	−5.7(3.2)	−1	2.4	2.2

B. Parities in ^{140}Ce

Spectra of vertical and horizontal coincidences for the ^{140}Ce target in the energy range from 6 to 7 MeV are shown in Fig. 5. Table III shows the resulting asymmetries of the analyzed peaks. Because of lack of statistics or superpositions with strong escape peaks some peaks could not be evaluated properly. The two groups of transitions with $E_\gamma = 6606, 6616$ keV and $E_\gamma = 6439, 6449, 6459$ keV appear as a doublet and a triplet, respectively. In Fig. 6 the asymmetries are compared to the polarization sensitivity of the clover detector. Since the degree of linear polarization of the transitions under consideration is $|P_\gamma| = 1$, the positive and negative sign corresponds to positive and negative parity of the excited state respectively. The errors of the polarization sensitivity are shown as shaded bands.

All asymmetries show negative signs leading to an assignment of electric character to the corresponding transitions.

As an estimate of the confidence level for this assignment the deviation of each data point from the $M1$ expectation value (given by the positive polarization sensitivity) is taken. These values, expressed in terms of the standard deviation of the individual data points, are given in Table III in the row labeled "Conf.". For a more accurate confidence analysis one has to take into account the nonvanishing error of the polarization sensitivity as well. Therefore, χ^2 values with respect to the positive polarization-sensitivity curve were calculated for all data points. Taking the errors of the polarization sensitivity and of the asymmetries of the data points as independent of

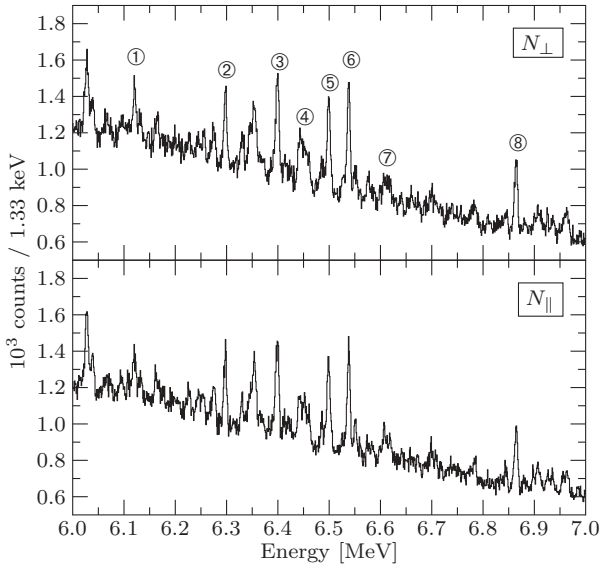

FIG. 5. Spectra of ^{140}Ce between 6 and 7 MeV of coincidences perpendicular and parallel to the reaction plane. The duration of the measurement was 290 h. Only peaks marked with number symbols were evaluated. See Fig. 6 and Table III for the results.

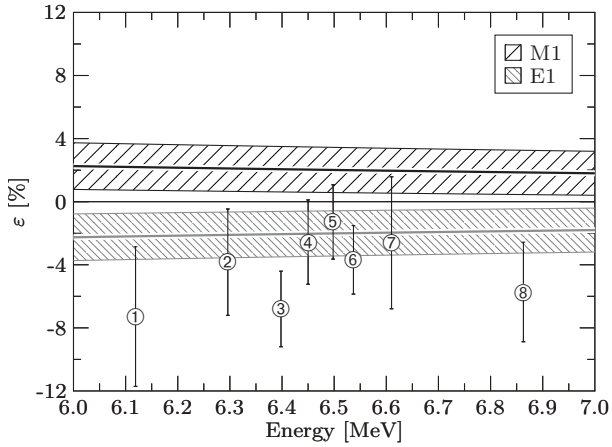

FIG. 6. Asymmetries of dipole transitions in ^{140}Ce between 6 and 7 MeV versus the values of the asymmetries expected for $E1$ and $M1$ transitions, respectively. The bands are obtained from the polarization-sensitivity analysis, see Sec. III A. For all transitions magnetic character can be excluded with confidence levels of at least 1σ, see text and Table III.

each other, the integrated probability distribution

$$P(\chi^2) = \int_0^{\chi^2} \frac{\exp(x^2/2)}{\sqrt{2\pi x^2}} dx^2 \qquad (12)$$

for finding a value up to χ^2 gives another quantitative measure of the confidence level for the exclusion of magnetic character. See Ref. [24] for details. The results are summarized in Table III. With both methods confidence levels are obtained which amount to at least 1σ and therefore support the assignment of negative parity to all states under consideration.

IV. SUMMARY AND CONCLUSION

The method of Compton polarimetry which is well established at energies of up to about 4 MeV was applied successfully in the energy region up to 7 MeV and allowed model-independent parity assignments. Negative parity was assigned to all of the examined states of ^{140}Ce in the region of the PDR at a confidence level of 1σ or better. The result that the states in this region show negative parity is in agreement with the expectation following from the observation for the even-even neighbor nucleus ^{138}Ba. Since the nonpopulation of the higher lying states via α scattering can therefore not be explained as a change in parity, it seems appropriate to refer to a splitting of the PDR. This splitting could be explained by a different isospin character of the two components, i.e., isoscalar and isovector character of the low-lying and the high-lying states, respectively. It is planned to further address this question with complementary measurements using different hadronic probes.

ACKNOWLEDGMENTS

We thank the KVI Groningen for lending us the clover detector. This work was supported by the Deutsche Forschungsgemeinschaft under contract SFB 634.

[1] U. Kneissl, H. H. Pitz, and A. Zilges, Prog. Part. Nucl. Phys. **37**, 349 (1996).
[2] U. Kneissl, N. Pietralla, and A. Zilges, J. Phys. G: Nucl. Part. Phys. **32**, R217 (2006).
[3] K. Govaert, F. Bauwens, J. Bryssinck, D. De Frenne, E. Jacobs, W. Mondelaers, L. Govor, and V. Y. Ponomarev, Phys. Rev. C **57**, 2229 (1998).
[4] T. Hartmann, M. Babilon, S. Kamerdzhiev, E. Litvinova, D. Savran, S. Volz, and A. Zilges, Phys. Rev. Lett. **93**, 192501 (2004).
[5] S. Volz, N. Tsoneva, M. Babilon, M. Elvers, J. Hasper, R.-D. Herzberg, H. Lenske, K. Lindenberg, D. Savran, and A. Zilges, Nucl. Phys. **A779**, 1 (2006).
[6] N. Ryezayeva, T. Hartmann, Y. Kalmykov, H. Lenske, P. von Neumann-Cosel, V. Y. Ponomarev, A. Richter, A. Shevchenko, S. Volz, and J. Wambach, Phys. Rev. Lett. **89**, 272502 (2002).
[7] D. Savran, M. Fritzsche, J. Hasper, K. Lindenberg, S. Müller, V. Y. Ponomarev, K. Sonnabend, and A. Zilges, Phys. Rev. Lett. **100**, 232501 (2008).
[8] N. Paar, D. Vretenar, E. Khan, and G. Colo, Rep. Prog. Phys. **70**, 691 (2007).
[9] N. Pietralla, Z. Berant, V. N. Litvinenko, S. Hartman, F. F. Mikhailov, I. V. Pinayev, G. Swift, M. W. Ahmed, J. H. Kelley, S. O. Nelson *et al.*, Phys. Rev. Lett. **88**, 012502 (2001).
[10] D. Savran, M. Babilon, A. M. van den Berg, M. N. Harakeh, J. Hasper, A. Matic, H. J. Wörtche, and A. Zilges, Phys. Rev. Lett. **97**, 172502 (2006).
[11] W. W. Eidson, J. G. Cramer, Jr., Phys. Rev. Lett. **9**, 497 (1962).
[12] P. Weigt, H. Hilbel, P. Gottel, R. Herzog, and E. Bodenstedt, Nucl. Instrum. Methods **57**, 295 (1967).
[13] K. E. Davies and W. D. Hamilton, Nucl. Instrum. Methods **59**, 1 (1968).
[14] E. Eube, J. Eberth, U. Eberth, H. Eichner, and V. Zobel, Nucl. Instrum. Methods **130**, 73 (1975).
[15] R. Bass, J. Idzko, H. Pelz, K. Stelzer, T. Weber, and R. Weniger, Nucl. Instrum. Methods **163**, 373 (1979).
[16] A. J. Ferguson, Nucl. Instrum. Methods **162**, 565 (1979).
[17] J. Simpson, P. A. Butler, and L. P. Ekström, Nucl. Instrum. Methods **204**, 463 (1983).
[18] R. D. Heil, B. Kasten, W. Scharfe, P. A. Butler, H. Friedrichs, S. D. Hoblit, U. Kneissl, S. Lindenstruth, M. Ludwig, G. Müller *et al.*, Nucl. Phys. **A506**, 223 (1990).
[19] C. Hutter, M. Babilon, W. Bayer, D. Galaviz, T. Hartmann, P. Mohr, S. Müller, W. Rochow, D. Savran, K. Sonnabend *et al.*, Nucl. Instrum. Methods A **489**, 247 (2002).
[20] K. Siegbahn, *Alpha-, Beta, and Gamma-Ray Spectroscopy* (North-Holland Publishing Company, Amsterdam, 1966).
[21] A. H. Wapstra, G. J. Nijgh, and R. van Lieshout, *Nuclear Spectroscopy Tables* (North-Holland Publishing Company, Amsterdam, 1959).
[22] L. W. Fagg and S. S. Hanna, Rev. Mod. Phys. **31**, 711 (1959).
[23] P. M. Jones, L. Wei, F. A. Beck, P. A. Butler, T. Byrski, G. Duchêne, G. de France, F. Hannachi, G. D. Jones, and B. Kharraja, Nucl. Instrum. Methods A **362**, 556 (1995).
[24] P. R. Bevington and D. K. Robinson, *Data Reduction and Error Analysis for Physical Sciences* (McGraw-Hill, New York, 1992), 2nd ed.